Metagenomic sequencing provides insights into the location of microbial detoxification in the gut of a small mammalian herbivore

Kevin D. Kohl[1,2], Kelly F. Oakeson[2], Teri J. Orr[2], Aaron W. Miller[2,3], Jennifer Sorensen Forbey[4], Caleb D. Phillips[5], Colin Dale[2], Robert B. Weiss[6], M. Denise Dearing[2]

[1]*Department of Biological Sciences, University of Pittsburgh, 4249 Fifth Ave., Pittsburgh, PA, 15260, USA*

[2] *Department of Biology, University of Utah, 257 South 1400 East, Salt Lake City, UT, 84112, USA*

[3] *Departments of Urology and Immunology, Cleveland Clinic Foundation, 9500 Euclid Ave, Cleveland, OH 44195*

[4] *Department of Biological Sciences, Boise State University, 1910 University Drive, Boise, Idaho 83725 USA*

[5] *Department of Biological Sciences, Texas Tech University, 2901 Main Street, Lubbock, TX, 79409*

[6] *Department of Human Genetics, University of Utah, 15 North 2030 East, Salt Lake City, UT, 84112, USA*

Corresponding Author:
Kevin Kohl – University of Pittsburgh
Kevin.d.kohl@gmail.com
ORCID: 0000-0003-1126-2949

Keywords: host-microbe interactions, oxalate, PICRUSt, terpenes, woodrat

Abstract – Microbial detoxification of plant defense compounds influences the use of certain plants as food sources by herbivores. The location of microbial detoxification along the gut could have profound influences on the distribution, metabolism, and tolerance to toxic compounds. Stephen's woodrats (*Neotoma stephensi*) specialize on juniper, which is heavily defended by numerous defensive compounds, such as oxalate, phenolics, and monoterpenes. Woodrats maintain two gut chambers harboring dense microbial communities: a foregut chamber proximal to the major site of toxin absorption, and a cecal chamber in their hindgut. We performed several experiments to investigate the location of microbial detoxification in the woodrat gut. First, we measured levels of toxins across gut chambers. Compared to food material, oxalate concentrations were immediately lower in the foregut chamber, while concentrations of terpenes remain high in the foregut, and are lowest in the cecal chamber. We also conducted metagenomic sequencing of the foregut and cecal chambers to compare microbial functions. We found that the majority of genes associated with detoxification functions were more abundant in the cecal chamber. However, some genes associated with degradation of oxalate and phenolic compounds were more abundant in the foregut. Thus, it seems that microbial detoxification may take place in various chambers depending on the class of chemical compound. We hypothesize that the location of microbial detoxification could impact the tolerance of animals to these compounds, which may have ecological and evolutionary consequences.

52 **INTRODUCTION**

53 Mammalian herbivores are often challenged by the consumption of toxic
54 plant secondary compounds (PSCs) that negatively impact their physiology in
55 various ways [1]. In response, mammalian herbivores have evolved myriad
56 adaptations to cope with dietary toxins, such as altered behavior, efflux pumps in
57 the gut, and enhanced liver detoxification [1]. Recently, we demonstrated that the
58 gut microbiota of herbivores also play an important role in allowing them to
59 consume PSCs [2]. However, it is still unclear where the process of microbial
60 detoxification occurs in the gut.

61 It has been proposed that microbial detoxification should occur early in the
62 gastrointestinal tract, to facilitate rapid degradation of PSCs and minimize the
63 potential for their absorption in the digestive tract. In fact, it has been hypothesized
64 that the rumen evolved first for detoxification and was later adopted for processes
65 of fermentation [3, 4]. Examples of animals in which foregut detoxification has been
66 documented for particular PSCs include reindeer (*Rangifer tarandus*; [5] that have
67 rumen communities that degrade usnic acid, a toxin produced by lichen, and
68 hoatzins (*Opisthocomus hoazin*), that maintain communities of microbes in their
69 foregut capable of metabolizing saponins [6]. There is also evidence of microbial
70 detoxification processes occurring in the hindguts of some animals. For example,
71 Sage-grouse (*Centrocercus urophasianus*), specialize on toxic sagebrush (*Artemsia*
72 spp.) and maintain a cecal microbiota enriched in detoxification genes [7].
73 Additionally, the hindguts of koalas (*Phascolarctos cinereus*) harbor microbes
74 capable of degrading phenolic PSCs [8]. Understanding the location of microbial

75 processes in the gut is likely to be important in the context of animal ecology. For
76 example, the location of fermentation (foregut vs hindgut), seems to facilitate or
77 constrain evolution of herbivore body size [9] and dietary niche breadth [10]. The
78 location of microbial detoxification could have similar impacts on animal ecology.

79 In contrast to many above described examples, woodrats (genus *Neotoma*)
80 are particularly interesting from a digestive standpoint as these herbivorous
81 rodents possess both a foregut chamber and a large cecal chamber in their hindgut.
82 Both the foregut and cecal chambers harbor dense communities of microbes and
83 high concentrations of volatile fatty acids [11], which are the microbial products of
84 fermentation. Following the hypothesis that the bovine rumen first evolved for
85 detoxification regarding the rumen [3, 4], we predict that microbial detoxification of
86 PSCs might occur prior to the small intestine in the woodrat gut such that the animal
87 experiences limited absorption and systemic exposure to toxic compounds.

88 To evaluate this hypothesis, we conducted a series of experiments focusing
89 on a species of woodrat with a highly specialized diet. Stephen's woodrat (*Neotoma*
90 *stephensi*) is a dietary specialist, with juniper (*Juniperus monosperma*) composing
91 ~90% of its diet [12]. Juniper defends itself from herbivory with various toxic
92 compounds, including monoterpenes [13], phenolics [14, 15], and oxalate [16]. We
93 have demonstrated that microbes aid in the detoxification of phenolics [2] and
94 oxalate in other woodrat species [17, 18]. For example, some populations of the
95 white-throated woodrat (*N. albigula*) specialize on cactus (*Opuntia* spp.), which is
96 rich in oxalate, but lacking in other defensive compounds. The foregut microbial
97 communities of these *N. albigula* contain several species of oxalate-degrading

98 microbes [19]. There has also been metagenomic evidence obtained from other
99 systems suggesting that microbes aid in the detoxification of terpenes (mountain
100 pine beetles: [20]; sage grouse: [7], as well as experimental work demonstrating the
101 detoxification function of the gut microbiota of pine weevils [21]). However, the
102 detoxification contribution of the microbiome has not been compared between the
103 foregut and hindgut in any wild vertebrate herbivore.

104 We addressed several questions within the woodrat-juniper system. First, we
105 measured concentrations of two classes of toxins (oxalate and monoterpenes)
106 across regions of the gut. We predicted that if detoxification is occurring proximally
107 in the gut, then toxins concentrations in the foregut would be significantly lower
108 compared to food material. Next, we conducted a series of metagenomic analyses to
109 inventory and compare the functions of microbial communities. We first compared
110 the metagenomes of foregut communities between the juniper specialist *N. stephensi*
111 and the cactus specialist *N. albigula* and predicted that if the foregut microbiota of *N.*
112 *stephensi* were specialized for detoxification of juniper, which contains oxalate,
113 monoterpenes, and phenolics, we would observe enrichment of detoxification genes
114 compared to the foregut of *N. albigula* that is exposed primarily to the oxalate in
115 cactus. We also compared the metagenomes of foregut and cecal chambers within *N.*
116 *stephensi* and predicted that the metagenome of the foregut chamber would be
117 enriched in detoxification genes compared to the cecal communities.
118
119
120

121 **MATERIALS AND METHODS**

122 All experiments below were approved by the University of Utah Institutional
123 Animal Care and Use Committee (IACUC) under protocols #12-12010 and #16-
124 02011.

125

126 *Toxin Levels Throughout the Gut*

127 We conducted a feeding trial on *N. stephensi* to document changes in toxin
128 concentrations across gut regions. Six individuals of *N. stephensi* were fed increasing
129 concentrations of *J. monosperma* (3 days on 25%, 3 days on 50%, 4 days on 75%).
130 On the last morning, animals were euthanized using isoflurane. Contents of each gut
131 region (foregut, stomach, small intestine, cecum, large intestine, feces) were
132 collected. A small portion of wet gut contents were placed in airtight headspace
133 autosampler vials and frozen at -20°C until analysis. Concentrations of individual
134 monoterpenes were determined using headspace gas chromatography with an
135 Agilent 7694 headspace sampler coupled with an Agilent 6890N gas chromatograph
136 (GC). One mL of headspace gas was injected into a J&W DB-5 capillary column (30
137 m × 250 μm × 0.25 μm). Operating conditions for the headspace sampler were: oven
138 temperature at 100°C, loop temperature at 110°C, transfer line temperature at
139 120°C, a vial equilibrium time of 20 min, a pressurization time of 0.20 min, a loop fill
140 time of 0.50 min, a loop equilibrium time of 0.20 min, and an injection time of 0.50
141 min. Operating conditions for the GC were: splitless injector at 250°C, flame
142 ionization detector at 300°C, oven temperature at 40°C for 2 min, then increasing
143 3°C/min to 60°C, then increasing 5°C/min to 120°C, then increasing 20°C/min to

144 300°C, and held at 300°C for 7 min. The make-up gas was nitrogen and the carrier
145 gas was helium. The inlet pressure was 80 kPa with a flow rate of 1.0 mL/min.
146 Retention times and peak areas of individual monoterpenes were calculated using
147 Agilent OpenLab version A.01.05. We verified the relative retention times of
148 individual monoterpenes using standards, and estimated the relative concentrations
149 of individual monoterpenes in the intestinal content material by comparing AUC of
150 peaks in diet or gut samples to AUC of a known volume of 10 mg/mL monoterpene
151 standards.

152 Remaining gut contents were placed in weighing boats and dried at 40°C for
153 two nights. The dried gut contents were then used to measure oxalate
154 concentrations using a previously established protocol [22]. Roughly 0.4g of dried
155 gut contents were ground and added to 5 mL of 6 N H_2SO_4 to solubilize the oxalate.
156 After 15 min, 25 ml of distilled water was added, and the entire solution was filtered
157 through grade 4 Whatman filter paper. The filtrate was brought up to a pH of 7 with
158 NaOH, and 0.1 g of $CaCl_2$ was added to precipitate the oxalate. The samples were
159 centrifuged and decanted. After centrifugation, a volume of distilled water equal to
160 that recovered after filtration was added, and the samples were titrated.

161

162 *Sample collection for metagenomics*

163 We compared the metagenomic sequencing results across species and gut
164 regions to investigate differential abundance of microbial functions. We collected
165 individuals of the cactus specialist *N. albigula*, from Castle Valley, UT, USA (38°30' N,
166 109°18' W). Individuals of *N. stephensi* (different individual from those described in

167 the experiment above) were collected from near Wupatki National Monument, AZ,
168 USA (35°30' N, 111°27' W). Animals were immediately transported back to the
169 University of Utah animal facility, provided with native diets: either cactus pads or
170 juniper overnight (for *N. albigula* and *N. stephensi*, respectively), and euthanized and
171 dissected on the following morning. Contents of the foregut chamber were collected
172 from three individuals of both species, and the contents of the cecal chamber were
173 collected from *N. stephensi*. We sequenced the metagenome of each sample
174 (described below), and conducted several comparisons. First, we compared the
175 foregut metagenomes of *N. albigula* and *N. stephensi*, with the prediction that the
176 foregut of *N. stephensi* would be enriched in genes associated with detoxification of
177 juniper, which contains more chemical classes of defensive compounds than cactus.
178 Second, we compared the metagenomes of foregut contents and cecal contents in *N.*
179 *stephensi* with the prediction that the abundance of detoxification genes would be
180 higher in the foregut to facilitate detoxification prior to the major site of absorption
181 in the small intestine.
182
183 *Comparative metagenomics*
184 Total DNA was isolated from foregut and cecal contents using MoBio
185 PowerFecal DNA extraction kit (MoBio, Carlsbad, California). Extracted DNA was
186 sent to Argonne National Laboratory for sequencing. Genomic DNA was sheared
187 using a Covaris Sonicator, to roughly 150 bp and metagenomic shotgun libraries
188 were prepared using the Illumina TruSeq DNA sequencing preparation kits.

189 Libraries were sequenced on the Illumina HiSeq2000 platform using a 2 x 100 bp
190 run and V3 chemistry, which resulted in overlapping sequences.

191 Metagenomic sequences were uploaded to the MG-RAST website [23].
192 Sequences were screened against the genome of *Arabidopsis thaliana* to remove
193 potential contamination from the plant-based diet. The reads were then filtered
194 using dynamic trimming with a quality threshold of 15, such that any sequences
195 with more than 5 low-quality bases were removed. Several foregut metagenomes
196 contained high abundances of sequences (~30-50%) identified as plant DNA, likely
197 resulting from the diet. Therefore, we partitioned our analysis by domain by
198 selecting sequences identified as bacteria using the non-redundant multi-source
199 protein annotation database, M5nr [24]. Abundances of non-plant eukaryotic and
200 archaeal sequences were too low for sufficient analysis. Sequences identified as
201 bacterial in origin were then annotated to identify putative functions using the
202 KEGG Orthology database [25, 26] with the following thresholds: (1) e-values < 1e-
203 5, (2) a minimum percent identity to database sequences of 60% and (3) a minimum
204 alignment length of 15 bases. We compared the abundances at Level 3 of the KEGG
205 hierarchical classification, as well as specific genes associated with "Xenobiotic
206 degradation and metabolism", "Geraniol degradation", and "Limonene and pinene
207 degradation". Abundances of functional categories were compared using JMP 12.0
208 (SAS Institute Inc.) using t-tests and the robust Response Screening function that
209 performs the Benjamini-Hochberg false discovery rate (FDR) correction for multiple
210 tests [27].

211 We also conducted specific comparisons of the abundances of several
212 detoxification genes: oxalyl-CoA decarboxylase, aryl alcohol dehydrogenase, and
213 several genes associated with terpene metabolism. The gene oxalyl-CoA
214 decarboxylase (*oxc*) degrades the compound oxalate. The gene aryl alcohol
215 dehydrogenase is upregulated in the woodrat foregut when individuals are fed diets
216 containing phenolic-rich resin from creosote bush [2]. Last, a number of genes
217 associated with the "Limonene and pinene degradation" are enriched or present in
218 the gut microbiota of specialist insect and avian herbivores that feed on terpene-rich
219 plants [7, 20]. We compared the abundances of these genes using JMP 12.0 (SAS
220 Institute Inc.) using pairwise t-tests (foregut *N. stephensi* vs. foregut *N. albigula*, and
221 *N. stephensi* foregut vs. cecum) with the Dunn's correction.
222
223 *Metagenome prediction*
224 We also conducted microbial inventories by sequencing the variable regions
225 1-3 of 16S rRNA gene following experimental and bioinformatic methods described
226 in detail elsewhere [28]. Taxonomic comparison of the communities between
227 foregut and cecal chambers has already been conducted with larger sample sizes
228 [11]. In the current study, we used 16S rRNA inventories to predict the
229 metagenomic content of gut samples using genomic inference via PICRUSt [29]. We
230 compared the relative abundances of functional categories between the shotgun
231 metagenomic and predicted metagenomics to assess if predictive profiling via
232 PICRUSt is informative for woodrat gut samples. First, we averaged the relative
233 abundances of functional categories within a sample type (foregut and cecum), and

234 transformed the relative abundances using a log(x+1) transformation. We then
235 conducted a linear regression between transformed PICRUSt abundances and
236 metagenomic abundances. We also plotted the relative abundances of functional
237 categories that exhibited the highest fold difference between the foregut and cecal
238 chambers to qualitatively inspect whether trends were similar for PICRUSt and
239 metagenomic data.
240
241 *Accession Numbers*
242 Metagenomic sequences can be found in the NCBI Short Read Archive (SRA)
243 database under BioProject PRJNA336354, and on MG-RAST under Metagenome
244 Project IDs mgp10174 and mgp10296. 16S rRNA sequences from the foregut and
245 cecal chambers of *N. stephensi* that were used in PICRUSt analyses can be found in
246 the SRA database under BioProject PRJNA449358.
247
248 **RESULTS**
249 *Concentrations of PSCs across the gut*
250 Water concentration varied over the length of the gut, with a significant
251 reduction in the large intestine (Fig. 2). Oxalate concentrations in the entire gut
252 were significantly less than in the food material (Fig 2; $P < 0.0001$). Oxalate
253 concentrations also varied significantly across gut regions ($P < 0.001$), and were
254 highest in the foregut and lowest in the stomach. Conversely, foregut concentrations
255 of monoterpenes were not significantly lower than the food material (Fig. 2; $P > 0.05$
256 for all). Concentrations of monoterpenes did vary across gut regions, with the

257 lowest concentrations always being in the cecum (Fig. 2; $P < 0.0001$ for all). In fact,
258 camphene and β-pinene were not detectable in any cecal samples.
259
260 *Metagenomic sequencing*
261 We obtained an average of 3.35 million reads per sample (± 517 thousand).
262 We first compared the bacterial metagenomes of foregut chambers from *N. stephensi*
263 (which specializes on juniper) and *N. albigula* (which specializes on cactus). There
264 were no functions that were significantly enriched in the foregut bacterial
265 metagenomes of *N. stephensi*. The foregut bacterial communities of *N. albigula* were
266 enriched in functions related to the metabolism of several amino acids and vitamin
267 B6 (Fig. 3). Further, when investigating detoxification genes, there were no
268 detectable differences between the two species.
269 We next searched for differential functions between the foregut and cecal
270 chambers of *N. stephensi*. The foregut bacterial metagenome was enriched in genes
271 associated with the metabolism of nucleotides (purines), amino acids (glutathione,
272 thiamine), vitamins (riboflavin, nicotinate, folate), and lipoic acid (Fig. 4A). The cecal
273 bacterial metagenome was enriched for genes associated with the metabolism of
274 starch and sucrose, as well as the biosynthesis of several essential amino acids (Fig.
275 4A). The cecum was also enriched in several functional categories related to
276 detoxification (drug metabolism, chloroalkane and chloroalkene degradation; Fig.
277 4A).
278 We also specifically investigated genes associated with "Xenobiotic
279 degradation and metabolism", "Geraniol degradation", and "Limonene and pinene

280 degradation". Here, the only gene enriched in the foregut was 4-oxalocrotonate
281 tautomerase, which was 24× more abundant in the foregut compared to the cecum
282 (Fig. 4B). There were 5 other detoxification genes that were significantly more
283 abundant in the cecum compared to the foregut chamber (Fig. 4B). Three of these
284 genes (carboxylesterase 2, hydroxyatrazine ethylaminohydrolase, and 2-
285 hydroxycyclohexanecarboxyl-CoA dehydrogenase) were 2-3× more abundant in the
286 cecal chambers compared to the foregut chambers. Two genes, anthraniloyl-CoA
287 monooxygenase and dehalogenases, were not detected in the foregut chambers, but
288 were present in the cecal chambers of the juniper-feeding *N. stephensi* (Fig. 4B).

289 Last, we focused on a subset of detoxification enzymes highlighted from
290 previous studies. The gene oxalyl-CoA decarboxylase, which is anticipated to
291 function in oxalate degradation, did not exhibit differential abundance between the
292 foregut chambers of *N. stephensi* and *N. albigula*. However, the abundance of this
293 gene was 4.5× higher in the foregut of *N. stephensi* compared to the cecum (Fig. 5).
294 Similarly, aryl-alcohol dehydrogenase, which is more abundant in the woodrat
295 foregut when animals are fed phenolic-rich creosote resin [2], did not exhibit
296 significant differences between the foregut chambers of *N. stephensi* or *N. albigula*,
297 but was 41× higher in the *N. stephensi* foregut compared to the cecum (Fig. 5). Last,
298 we investigated several genes in the "Limonene and pinene degradation" pathway
299 that are enriched in other herbivores that feed on terpene-rich plants [7, 20, 21].
300 Enoyl-CoA hydratase (E.C. 4.2.1.17) was more abundant in the foregut of *N.*
301 *stephensi* compared to *N. albigula*, with no difference between the foregut and cecal
302 chambers of *N. stephensi* (Fig. 5). Additionally, aldehyde dehydrogenase (E.C.

303 1.2.1.3) exhibited no difference between the foregut chambers of *N. stephensi* and *N.*
304 *albigula,* but was 2.5× more abundant in the cecal chambers of *N. stephensi* (Fig. 5).
305 We found a significant positive relationship between the relative abundances
306 of functional categories as estimated by PICRUSt and determined by metagenomic
307 sequencing (Fig. 6; foregut: $R^2 = 0.49$, slope = 0.922 ± 0.074, $P < 0.0001$; cecum: $R^2 =$
308 0.51, slope = 0.978 ± 0.072, $P < 0.0001$). Some functional categories, such as those
309 representing 'Peptidases' and 'Amino acid Related Enzymes', were not well
310 predicted by PICRUSt, in that they were present on the x-axis (predicted to be
311 present by PICRUSt but not detected by metagenomic sequencing). However,
312 categories that exhibited the greatest fold-differences between the two chambers
313 were also predicted to differ by PICRUSt (Fig. 6; with the exception of Starch and
314 Sucrose Metabolism).
315
316 **DISCUSSION**
317 Here, we investigated the nature and location of microbial detoxification in
318 the guts of Stephen's woodrat, a juniper specialist. The location of detoxification
319 within the gut seems to vary depending on the chemical class of defensive
320 compounds. We discuss our findings below, as well as the potential ecological and
321 evolutionary consequences of foregut vs hindgut detoxification by the microbiome.
322 We first compared concentrations of PSCs along the length of the
323 gastrointestinal tract. We predicted that if toxins were metabolized early in the gut,
324 their concentrations in the foregut chamber would be lower than those measured in
325 food material, similar to what has been observed for usnic acid in the reindeer

326 rumen [5]. This was observed in the case of oxalate, where foregut concentrations
327 were roughly a third of those measured in the diet. Since oxalate is detected only at
328 very low levels in the urine of woodrats [16] and mammals do not produce the
329 necessary oxalate-degrading enzymes [30], it seems that oxalate is detoxified
330 efficiently by microbes in the foregut. Conversely, terpene concentrations in the
331 foregut were the same as those measured in food material, suggesting that the
332 foregut is not a significant site for detoxification. Instead, concentrations of terpenes
333 were lowest in the cecum, where some terpene compounds were not even detected.
334 These results are similar to those observed in sage-grouse, where terpene
335 concentrations are also lowest in the cecal chambers [31]. *Neotoma stephensi* has
336 physiological adaptations that reduce terpene absorption in the gut [32], perhaps
337 allowing terpene metabolism to be delayed until the food reaches the cecum. In the
338 case of terpenes, concentrations increased in the large intestine compared to the
339 cecum. While this change seems puzzling, we hypothesize that the selective
340 absorption of water in this gut region results in higher concentrations of toxins.
341 Further experiments, perhaps using radiolabeled compounds, are needed to
342 understand the routes of absorption and detoxification of these compounds in
343 different regions of the woodrat digestive system.

344 Interestingly, we did not observe many differences related to detoxification
345 between the foregut microbial metagenomes of *N. stephensi* and *N. albigula*, even
346 though these two host species feed on different diets with contrasting chemical
347 profiles. It could be that the foregut microbiome offers broad detoxification
348 capacities, while cecal microbial communities are more specialized. That being said,

349 we did observe a higher abundance of enoyl-CoA hydratase in the foregut of *N.*
350 *stephensi* compared to *N. albigula*. This gene plays a role in the ability for microbes
351 to degrade terpenes [33], and is enriched in the gut metagenomes of sage-grouse [7]
352 and mountain pine beetles [20]. Thus, there may be some functional enrichment for
353 detoxification in the foregut of *N. stephensi*.

354 Within *N. stephensi*, the foregut and cecal microbial communities appear to
355 provide different detoxification functions. In the foregut, we observed higher
356 abundance of the gene 4-oxalocrotonate tautomerase, which is involved in the
357 degradation of aromatic hydrocarbons by bacteria [34]. The foregut also had higher
358 abundances of the gene oxalyl-CoA decarboxylase, which degrades oxalate, and aryl-
359 alcohol dehydrogenase, which degrades aromatic hydrocarbons. The abundance of
360 aryl-alcohol dehydrogenase increases in the foregut of another woodrat species (*N.*
361 *lepida*) when animals are fed diets containing phenolic PSCs [2] and thus may be an
362 important enzyme that is provided by the foregut microbial community .

363 We also obtained evidence for enrichment of detoxification enzymes in the
364 cecal chamber. Higher-level gene categories, such as 'Drug Metabolism' and
365 'Chloroalkane and Chloroalkene Degradation' were more abundant in the cecal
366 chambers than the foregut. Specifically, the cecum was enriched for genes such as
367 hydroxyatrazine ethylaminohydrolase, which deaminates or dechlorinates triazine
368 compounds [35, 36], and anthraniloyl-CoA monooxygenase, which plays a role in
369 the catabolism of aromatic compounds [37]. Additionally, the aldehyde
370 dehydrogenase gene was significantly more abundant in the cecum. This gene is
371 annotated as a component of the 'Limonene and Pinene Degradation' pathway, and

372 is found to be enriched in the gut metagenomes of sage-grouse [7] and mountain
373 pine beetles [20].

374 Finally, we tested whether predictive profiling of metagenomics based on
375 16S rRNA sequences is appropriate for woodrat gut samples. We found a significant
376 relationship between the relative abundances of functional categories as estimated
377 by PICRUSt and determined by metagenomic sequencing. Additionally, results for
378 PICRUSt and metagenomics were consistent for some of the categories that
379 exhibited the largest differences between the two chambers. However, PICRUSt did
380 not predict all of the categories accurately. Many functional categories (e.g.
381 'Peptidases' and "Amino acid Related Enzymes') were predicted to be present by
382 PICRUSt analysis, but were not detected by metagenomic sequencing. Interestingly,
383 the gut microbial communities of herbivores tend to have lower abundances of
384 genes encoding protease relative to carnivores, likely to conserve these nutrients on
385 a low protein diet [38]. Thus, the use of predictive metagenomic profiling may not
386 always be feasible for non-model systems, especially given that most microbial
387 genomes used for predictive profiling are from the human gut. Indeed, PICRUSt
388 works significantly better for human samples than for samples from nonhuman
389 mammalian guts [29]. The sequencing of additional genomes from nonhuman
390 mammals would help to improve the accuracy of programs like PICRUSt in non-
391 model systems. It seems that results from predicting profiling in non-model systems
392 should perhaps be verified with other methods, such as quantitative PCR.

393 Overall, we hypothesized that microbial detoxification should occur
394 proximally in the gastrointestinal tract, so as to facilitate degradation of PSCs before

395 they would be absorbed later in the gut. However, it seems that detoxification
396 processes may be spatially structured along the length of the gut. The evidence for
397 foregut detoxification is strongest for oxalate, where abundances of the
398 detoxification enzyme (oxalyl-CoA decarboxylase) were high, and concentrations of
399 oxalate were already much lower than in food material, and abundances of
400 potentially oxalate-degrading bacteria are highest [19]. Terpene degradation may
401 occur in the cecal chamber, where abundances of terpene-degradation genes were
402 higher, and concentrations of terpenes were at their lowest. It is somewhat puzzling
403 why this spatial arrangement would exist, given that terpenes are absorbed very
404 rapidly due to their small size and high lipophilicity [32]. However, *N. stephensi*
405 exhibits lower terpene absorption than other woodrat species [32], resulting in
406 relatively higher terpene exposure and resultant detoxification by microbial
407 communities in the hindgut. Laboratory rats are able to excrete ~25% of absorbed
408 monoterpenes back into the gut lumen through the biliary duct [39], an excretion
409 route that may be enhanced in a specialist herbivore such as *N. stephensi*. This
410 excretion route may facilitate further microbial degradation of terpenes in the
411 hindgut. While we did not measure concentrations of phenolics through the gut,
412 various genes associated with degrading aromatic hydrocarbons were enriched in
413 both the foregut and cecum. Phenolics can bind to dietary protein and digestive
414 enzymes, thus limiting nutrient availability [40]. Therefore, foregut detoxification of
415 phenolics would be beneficial for avoiding the anti-nutritive effects of PSCs. Again,
416 labeled chemicals to trace sites of absorption, excretion, and metabolism would
417 enhance our understanding of the location of these processes.

418 The location of detoxification within the gut could have important ecological
419 and evolutionary implications for plants and herbivores. For example, when
420 comparing several species of rodents, only those with foregut chambers were able
421 to metabolize significant amounts of oxalate [41]. Thus, evolution of this chamber
422 may be important for the ability to consume oxalate-rich plants. Consumption of
423 plant toxins might also drive changes in gut anatomy to enhance detoxification by
424 facilitating a longer duration of residency in various gut chambers. For example,
425 woodrats feeding on phenolic-rich oak exhibit an increase in cecal size [42], which
426 could be driven by increased fiber content of oak or to facilitate the detoxification of
427 PSCs. Interestingly, supplementing diets with isolated phenolic compounds causes
428 an increase in cecal size in lab rats [43]. Alterations of the size or function of gut
429 chambers in response to toxins could have implications for dietary niche breadth or
430 energetics. In herbivorous birds, there is evidence suggesting that microbial
431 detoxification occurs in both foregut [6] and hindgut chambers [7]. The guts of birds
432 are under strong selective pressure to be small so as to facilitate flight [44], and thus
433 sites of microbial detoxification may be especially important in these species.
434 Studies on additional and phylogenetically diverse herbivores and classes of PSCs
435 may help us to better understand the importance of microbial detoxification in the
436 gut, and how the spatial arrangement of these processes contribute to animal
437 morphology, performance, ecology, and evolution.
438
439
440

Acknowledgements – We would like to thank Madelina James and KayLene Yamada for helping with feeding trials and Chelsea Merriman for analysis of monoterpenes. Funding for this study was provided by the National Science Foundation (Doctoral Dissertation Improvement Grant, DEB 1210094, to M.D.D. and K.D.K.; DEB 1342615 to M.D.D.; DEB-1146194 to JSF; and DBI 1400456 to K.D.K).

480 **References**

481

482 1. Dearing MD, Foley WJ, McLean S (2005) The influence of plant secondary
483 metabolites on the nutritional ecology of herbivorous terrestrial vertebrates
484 Ann Rev Ecol Evol Syst 36: 169-185.
485 2. Kohl KD, Weiss RB, Cox J, Dale C, Dearing MD (2014) Gut microbes of
486 mammalian herbivores facilitate intake of plant toxins. Ecol Lett 17: 1238-
487 1246.
488 3. Hume ID, Warner ACI (1980) Evolution of microbial digetion in mammals. In:
489 Ruckebusch, Y, Thivend, P (eds.) Digestive Physiology and Metabolism in
490 Ruminants. MTD Press, Lancaster, pp. 665-684
491 4. Mackie RI (2014) Mutualistic fermentative digestion in the gastrointestinal
492 tract: diversity and evolution. Integr Comp Biol 42: 319-326.
493 5. Sundset MA, Barboza PS, Green TK, Folkow LP, Blix AS, Mathiesen SD (2010)
494 Microbial degradation of usnic acid in the reindeer rumen.
495 Naturwissenschaften 97: 273-278.
496 6. Garcia-Amado MA, Michelangeli F, Gueneau P, Perez ME, Dominguez-Bello
497 MG (2007) Bacterial detoxification of saponins in the crop of the avian
498 foregut fermenter *Opisthocomus hoazin*. J Anim Feed Sci 16: 82-85.
499 7. Kohl KD, Connelly JW, Dearing MD, Forbey JS (2016) Microbial detoxification
500 in the gut of a specialist avian herbivore, the Greater Sage-Grouse. FEMS
501 Microbiol Lett 363: fnw144.

502 8. Osawa R (1992) Tannin-protein complex-degrading enterobacteria isolated
503 from the alimentary tracts of koalas and a selective medium for their
504 enumeration. Appl Environ Microbiol 58: 1754-1759.
505 9. Clauss M, Frey R, Kiefer B, Lechner-Doll M, Loehlein W, Polster C, Rössner GE,
506 Streich WJ (2003) The maximum attainable body size of herbivorous
507 mammals: morphophysiological constraints on foregut, and adaptations of
508 hindgut fermenters. Oecologia 136: 14-27.
509 10. Alexander RM (1991) Optimization of gut structure and diet for higher
510 vertebrate herbivores. Phil Trans R Soc 333: 249-255.
511 11. Kohl KD, Miller AW, Marvin JE, Mackie R, Dearing MD (2014) Herbivorous
512 rodents (*Neotoma* spp.) harbour abundant and active foregut microbiota.
513 Environ Microbiol 16: 2869-2878.
514 12. Vaughan TA (1982) Stephen's woodrat, a dietary specialist. J Mammal 63: 53-
515 62.
516 13. Schwartz CC, Nagy JG, Regelin WL (1980) Juniper oil yield, terpenoid
517 concentration, and antimicrobial effects on deer. J Wildl Manage 44: 107-113.
518 14. Dearing MD, McLister JD, Sorensen JS (2005) Woodrat (*Neotoma*) herbivores
519 maintain nitrogen balance on a low-nitrogen, high-phenolic forage, *Juniperus*
520 *monosperma*. J Comp Physiol B 175: 349-355.
521 15. Holechek JL, Munshikpu L, Saiwana L, Nunez-Hernandez G, Valdez R, Wallace
522 JD, Cardenas M (1990) Influences of six shrub diets varying in phenol content
523 on intake and nitrogen retention by goats. Trop Grassl 24: 93-98.

524 16. Justice KE (1985) Oxalate digestibility in *Neotoma albigula* and *Neotoma*
525 *mexicana*. Oecologia 67: 231-234.
526 17. Miller AW, Oakeson KF, Dale C, Dearing MD (2016) Microbial community
527 transplant results in increased and long-term oxalate degradation. Microb
528 Ecol 72: 470-478.
529 18. Miller AW, Dale C, Dearing MD (2017) The induction of oxalate metabolism in
530 vivo is more effective with functional microbial communities than with
531 functional microbial species. mSystems 2: e00088-00017.
532 19. Miller AW, Kohl KD, Dearing MD (2014) The gastrointestinal tract of the
533 white-throated woodrat (Neotoma albigula) harbors distinct consortia of
534 oxalate-degrading bacteria. Appl Environ Microbiol 80: 1595-1601.
535 20. Adams AS, Aylward FO, Adams SM, Erbilgin N, Aukema BH, Currie CR, Suen G,
536 Raffa KF (2013) Mountain pine beetles colonizing historical and naive trees
537 are associated with a bacterial community highly enriched in genes
538 contributing to terpene metabolism. Appl Environ Microbiol 79: 3468-3475.
539 21. Berasategui A, Salem H, Paetz C, Santoro M, Gershenzon J, Kaltenpoth M,
540 Schmidt A (2017) Gut microbiota of the pine weevil degrades conifer
541 diterpenes and increases insect fitness. Mol Ecol 26: 4099-4110.
542 22. Miller AW, Oakeson KF, Dale C, Dearing MD (2016) Effect of dietary oxalate
543 on the gut microbiota of the mammalian herbivore *Neotoma albigula*. Appl
544 Environ Microbiol 82: 2669-2675.
545 23. Meyer F, Paarmann D, D'Souza M, Olson R, Glass EM, Kubal M, Paczian T,
546 Rodriguez A, Stevens R, Wilke A, Wilkening J, Edwards RA (2008) The

547 metagenomics RAST server–a public resource for the automatic phylogenetic
548 and functional analysis of metagenomes. BMC Bioinformatics 9: 386.
549 24. Wilke A, Harrison T, Wilkening J, Field D, Glass EM, Kyrpides N, Mavrommatis
550 K, Meyer F (2012) The M5nr: a novel non-redundant database containing
551 protein sequences and annotations from multiple sources and associated
552 tools. BMC Bioinformatics 13: 141.
553 25. Kanehisa M, Sato Y, Kawashima M, Furumichi M, Tanabe M (2016) KEGG as a
554 reference resource for gene and protein annotation. Nucleid Acids Res 44:
555 D457-D462.
556 26. Kanehisa M, Goto S (2000) KEGG: Kyoto Encyclopedia of Genes and Genomes.
557 Nucleid Acids Res 28: 27-30.
558 27. Benjamini Y, Hochberg Y (1995) Controlling the false discovery rate: a
559 practical and powerful approach to multiple testing. J R Soc Stat Soc B 57:
560 289-300.
561 28. Phillips CD, Hanson J, Wilkinson JE, Koenig L, Rees E, Webala P, Kingston T
562 (2017) Microbiome structural and functional interactions across host dietary
563 niche space. Integr Comp Biol 57: 743-755.
564 29. Langille MGI, Zaneveld J, Caporaso JG, McDonald D, Knights D, Reyes JA,
565 Clemente JC, Burkepile DE, Thurber RLV, Knight R, Beiko RG, Huttenhower C
566 (2013) Predictive functional profiling of microbial communities using 16S
567 rRNA marker gene sequences. Nat Biotechnol 31: 814-821.
568 30. Miller AW, Dearing MD (2013) The metabolic and ecological interactions of
569 oxalate-degrading bacteria in the mammalian gut. Pathogens 2: 636-652.

570 31. Kohl KD, Pitman E, Robb BC, Connelly JW, Dearing MD, Forbey JS (2015)
571 Monoterpenes as inhibitors of digestive enzymes and counter-adaptations in
572 a specialist avian herbivore. J Comp Physiol B 185: 425-434.
573 32. Sorensen JS, Turnbull CA, Dearing MD (2004) A specialist herbivore
574 (*Neotoma stephensi*) absorbs fewer plant toxins than does a generalist
575 herbivore (*Neotoma albigula*). Physiol Biochem Zool 77.
576 33. Iurescia S, Marconi AM, Tofani D, Gambacorta A, Paternò A, Devirgiliis C, van
577 der Werf MJ, Zennaro E (1999) Identification and sequencing of β-myrcene
578 catabolism genes from *Pseudomonas* sp. strain M1. Appl Environ Microbiol
579 65: 2871-2876.
580 34. Harayama S, Timmis KN (1989) Catabolism of aromatic hydrocarbons by
581 *Pseudomonas*. In: Hopwood, DA, Chater, KF (eds.) Genetics of Bacterial
582 Diversity. Academic Press, London, pp. 152-175
583 35. Boundy-Mills K, de Souza ML, Mandelbaum RM, Wackett LP, Sadowsky MJ
584 (1997) The atzB gene of *Pseudomonas* sp. strain ADP encodes the second
585 enzyme of a novel atrazine degradation pathway. Appl Environ Microbiol 63:
586 916-923.
587 36. Seffernick JL, Shapir N, Schoeb M, Johnson G, Sadowsky MJ, Wackett LP
588 (2002) Enzymatic degradation of chlorodiamino-s-triazine. Appl Environ
589 Microbiol 68: 4672-4675.
590 37. Carmona M, Zamarro MT, Blázquez B, Durante-Rodríguez G, Juárez JF,
591 Valderrama JA, Barragán MJ, Garcia JL, Díaz E (2009) Anaerobic catabolism of

592 aromatic compounds: a genetic and genomic view. Microbiol Mol Biol Rev 73:
593 71-133.
594 38. Muegge BD, Kuczynski J, Knights D, Clemente JC, González A, Fontana L,
595 Henrissat B, Knight R, Gordon JI (2011) Diet drives convergence in gut
596 microbiome functions across mammalian phylogeny and within humans.
597 Science 332: 970-974.
598 39. Igimi H, Nishimura M, Kodama R, Ide H (1973) Studies on the metabolism of
599 d-limonene (p-mentha-1,8-diene): I. the absorption, distribution and
600 excretion of d-limonene in rats. Xenobiotica 4: 77-84.
601 40. Min BR, Barry TN, Attwood GT, McNabb WC (2003) The effect of condensed
602 tannins on the nutrition and health of ruminants fed fresh temperate forages:
603 a review. Anim Feed Sci Technol 106: 3-19.
604 41. Shirley EK, Schmidt-Nielsen K (1967) Oxalate metabolism in the pack rat,
605 sand rat, hamster, and white rat. J Nutr 91: 496-502.
606 42. Skopec MM, Haley S, Torregrossa A-M, Dearing MD (2008) An oak (Quercus
607 agrifolia) specialist (*Neotoma macrotis*) and a sympatric generalist (Neotoma
608 lepida) show similar intakes and digestibilities of oak. Physiol Biochem Zool
609 81: 426-433.
610 43. Zduńczyk Z, Juśkiewicz J, Estrella I (2006) Cecal parameters of rats fed diets
611 containing grapefruit polyphenols and inulin as single supplements or in a
612 combination. Nutrition 22: 898-904.
613 44. Price ER, Brun A, Caviedes-Vidal E, Karasov WH (2015) Digestive adaptations
614 of aerial lifestyles. Physiol 30: 69-78.

615 **Figure Legends**

616

617 **Fig. 1.** Concentrations of water and toxins across gut regions. The dotted line on
618 toxin graphs represents concentrations as measured in the food material presented
619 to woodrats. Points represent means ± 1 s.e.m.

620

621 **Fig. 2.** Functional categories (KEGG Level 3) that differed significantly between the
622 foregut metagenomes of *N. albigula* and *N. stephensi.* Bars represent means ± 1
623 s.e.m.

624

625 **Fig 3.** Differences in the metagenomic content of the foregut and cecal chambers of
626 *N. stephensi.* Bars represent means ± 1 s.e.m. A) Functional categories (KEGG Level
627 3) that differed significantly in abundance between the foregut and cecal
628 metagenomes. B) Detoxification genes that differed significantly in abundance
629 between the foregut and cecal metagenomes.

630

631 **Fig. 4.** Relative abundances of specific detoxification enzyme genes associated with
632 *a priori* hypotheses from other systems (see Methods). Bars represent means ± 1
633 s.e.m. Relative abundances were compared using t-tests (foregut *N. stephensi* vs.
634 foregut *N. albigula*, and *N. stephensi* foregut vs. cecum) with the Dunn's correction.

635

636

637 **Fig. 5. A)** A comparison of predictive profiling by PICRUSt and metagenomic data.
638 **B)** Bar graphs depict the functional categories that exhibited the highest fold-
639 differences between the foregut and cecal metagenomes. Bars represent means ± 1
640 s.e.m.
641

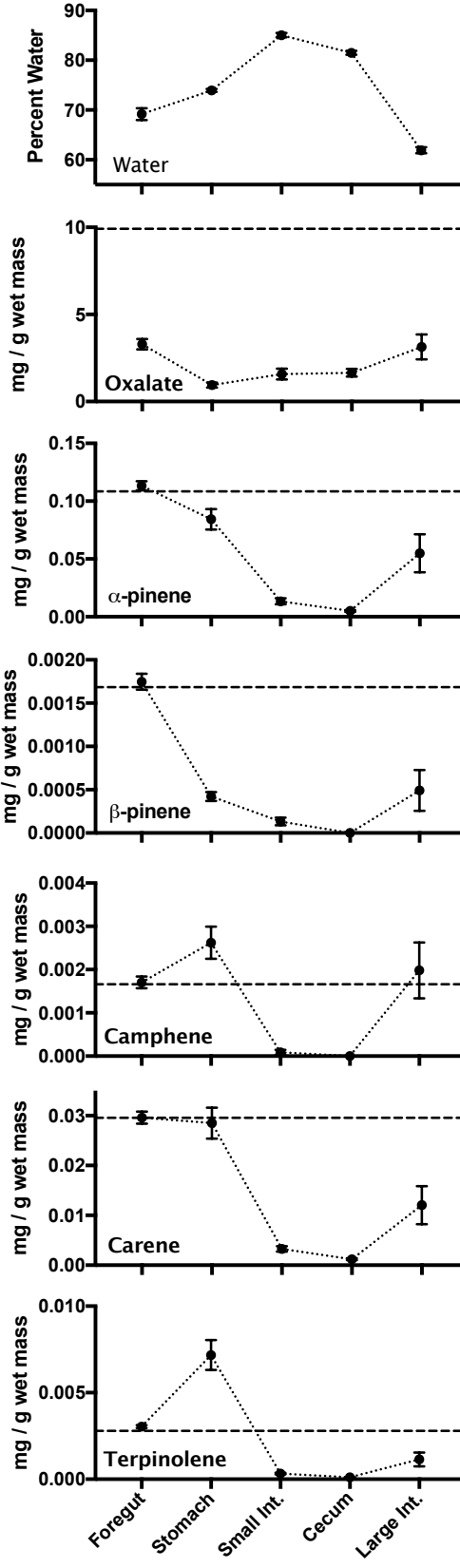
Percent Water
90
80
70
60
Water
mg / g wet mass
10
5
0
Oxalate
mg / g wet mass
0.15
0.10
0.05
0.00
α-pinene
mg / g wet mass
0.0020
0.0015
0.0010
0.0005
0.0000
β-pinene
mg / g wet mass
0.004
0.003
0.002
0.001
0.000
Camphene
mg / g wet mass
0.03
0.02
0.01
0.00
Carene
mg / g wet mass
0.010
0.005
0.000
Terpinolene
Foregut
Stomach
Small Int.
Cecum
Large Int.

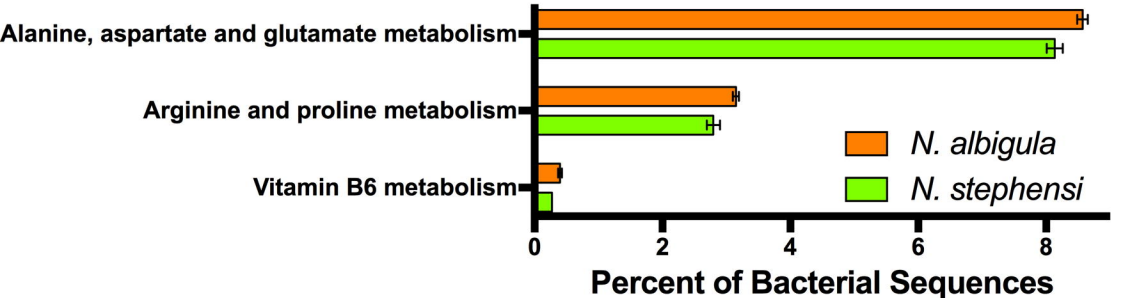
Alanine, aspartate and glutamate metabolism
Arginine and proline metabolism
Vitamin B6 metabolism
N. albigula
N. stephensi
0
2
4
6
8
Percent of Bacterial Sequences

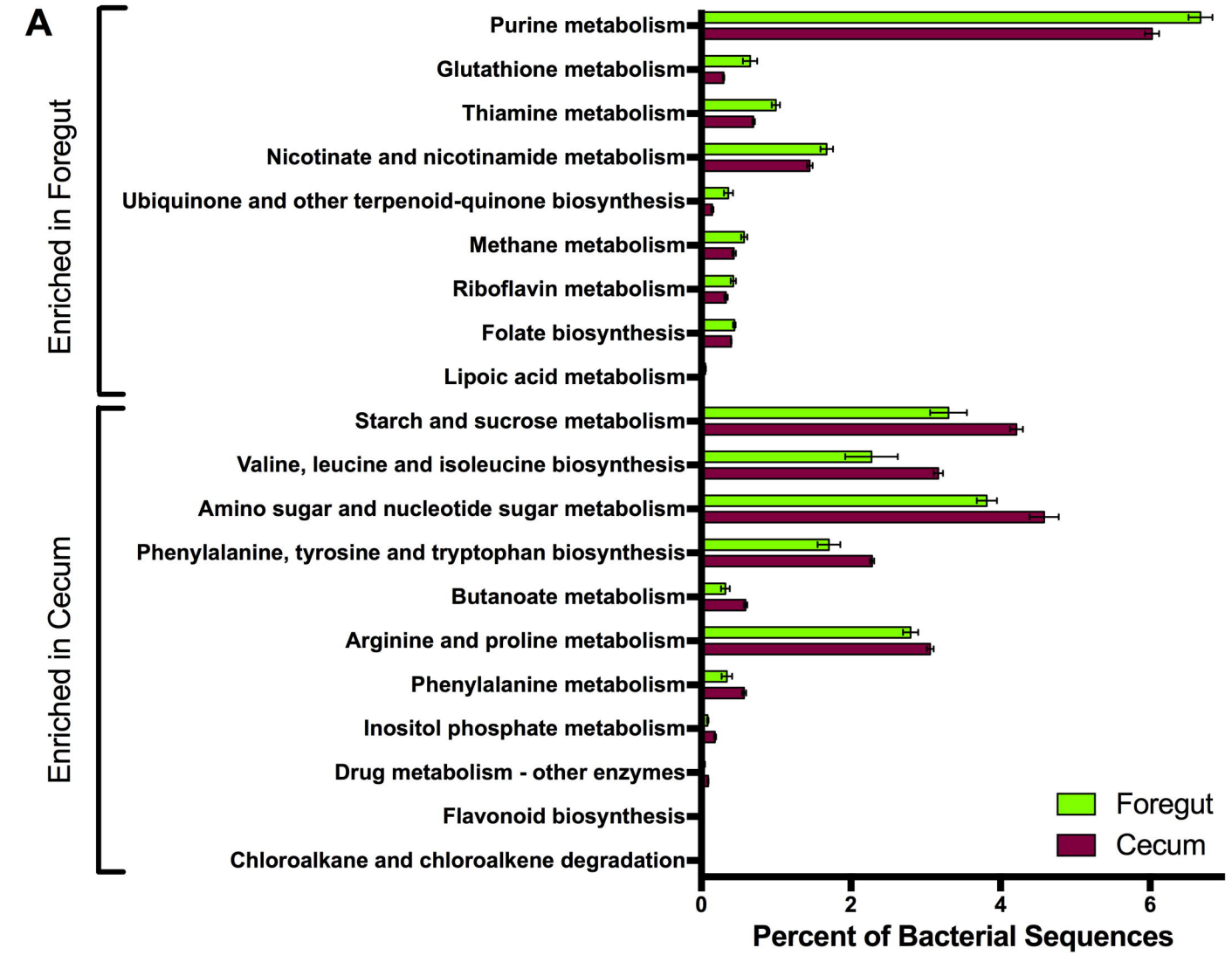
A
Enriched in Foregut
Enriched in Cecum
Purine metabolism
Glutathione metabolism
Thiamine metabolism
Nicotinate and nicotinamide metabolism
Ubiquinone and other terpenoid-quinone biosynthesis
Methane metabolism
Riboflavin metabolism
Folate biosynthesis
Lipoic acid metabolism
Starch and sucrose metabolism
Valine, leucine and isoleucine biosynthesis
Amino sugar and nucleotide sugar metabolism
Phenylalanine, tyrosine and tryptophan biosynthesis
Butanoate metabolism
Arginine and proline metabolism
Phenylalanine metabolism
Inositol phosphate metabolism
Drug metabolism - other enzymes
Flavonoid biosynthesis
Chloroalkane and chloroalkene degradation
Foregut
Cecum
0
2
4
6
Percent of Bacterial Sequences

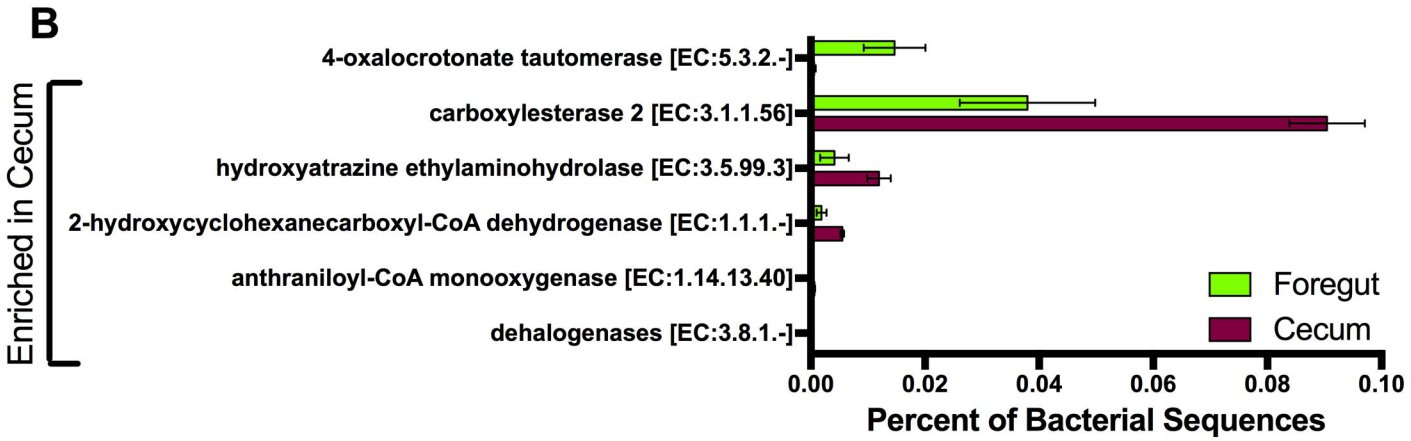
B
Enriched in Cecum
4-oxalocrotonate tautomerase [EC:5.3.2.-]
carboxylesterase 2 [EC:3.1.1.56]
hydroxyatrazine ethylaminohydrolase [EC:3.5.99.3]
2-hydroxycyclohexanecarboxyl-CoA dehydrogenase [EC:1.1.1.-]
anthraniloyl-CoA monooxygenase [EC:1.14.13.40]
dehalogenases [EC:3.8.1.-]
Foregut
Cecum
0.00
0.02
0.04
0.06
0.08
0.10
Percent of Bacterial Sequences

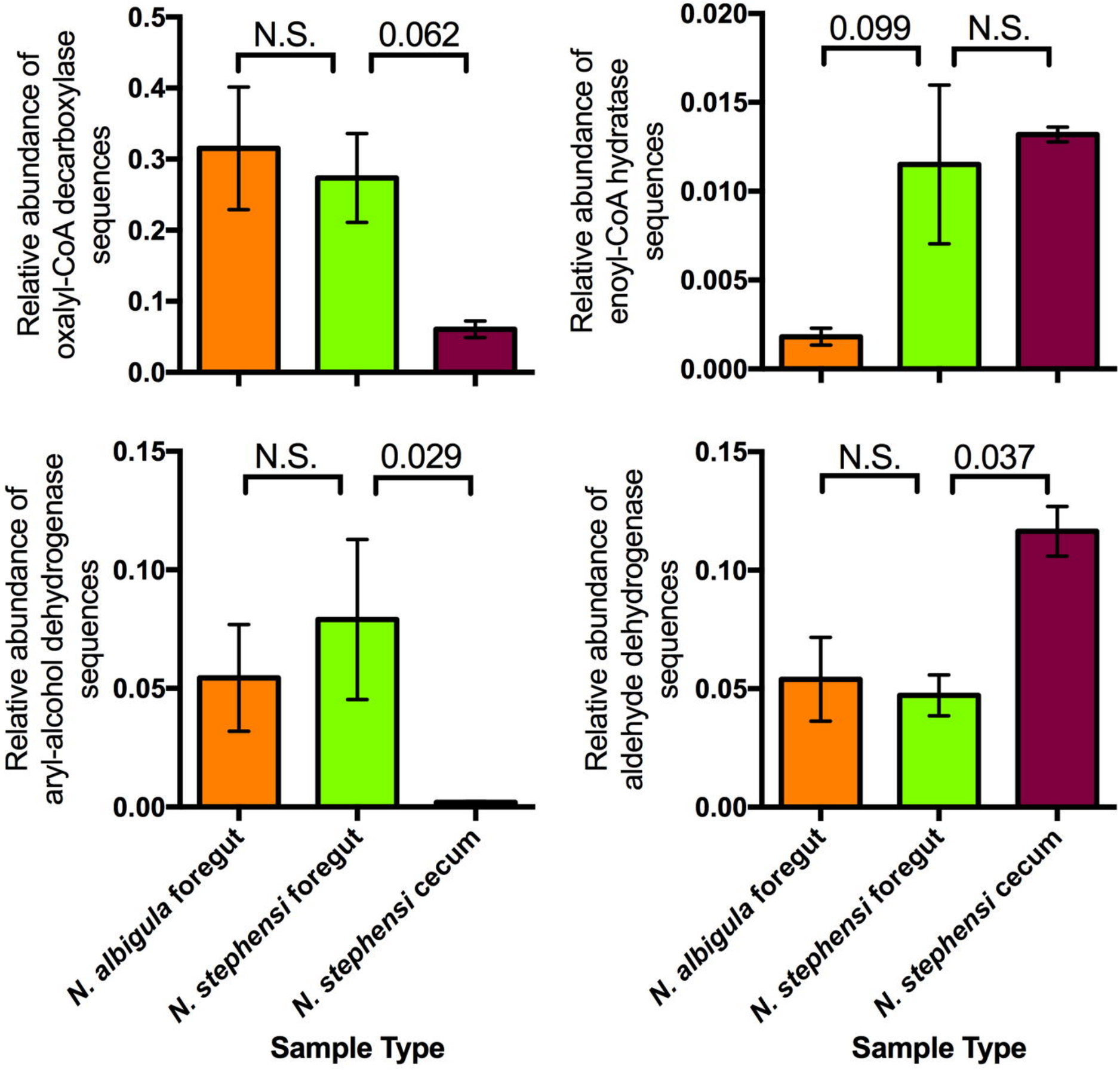
Relative abundance of oxalyl-CoA decarboxylase sequences
0.5
0.4
0.3
0.2
0.1
0.0
N.S.
0.062
Relative abundance of enoyl-CoA hydratase sequences
0.020
0.015
0.010
0.005
0.000
0.099
N.S.
Relative abundance of aryl-alcohol dehydrogenase sequences
0.15
0.10
0.05
0.00
N.S.
0.029
Relative abundance of aldehyde dehydrogenase sequences
0.15
0.10
0.05
0.00
N.S.
0.037
N. albigula foregut
N. stephensi foregut
N. stephensi cecum
Sample Type
N. albigula foregut
N. stephensi foregut
N. stephensi cecum
Sample Type

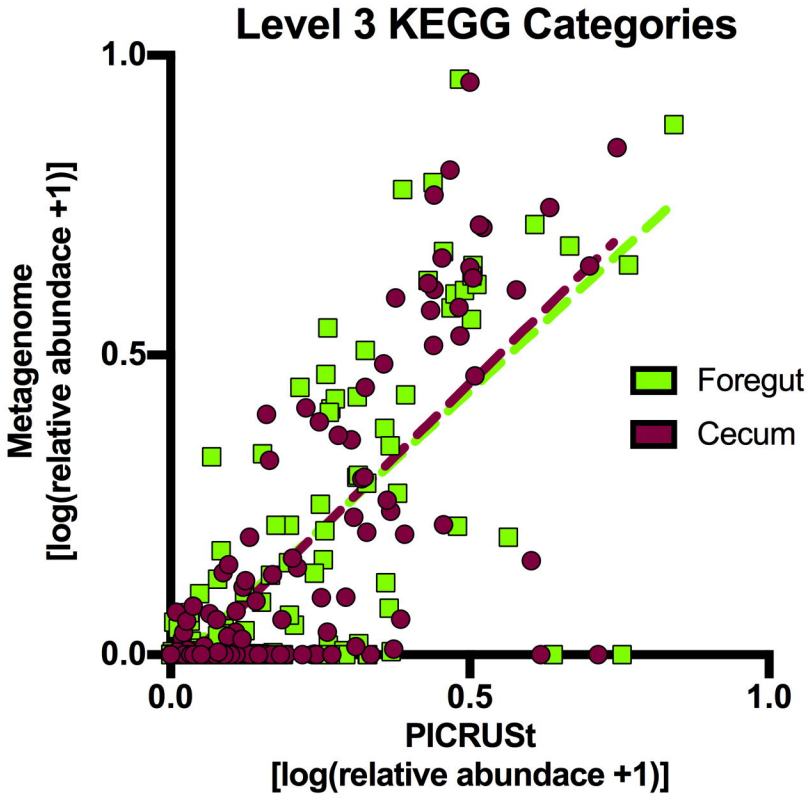
Level 3 KEGG Categories
Metagenome
[log(relative abundace +1)]
1.0
0.5
0.0
0.0
0.5
1.0
PICRUSt
[log(relative abundace +1)]
Foregut
Cecum

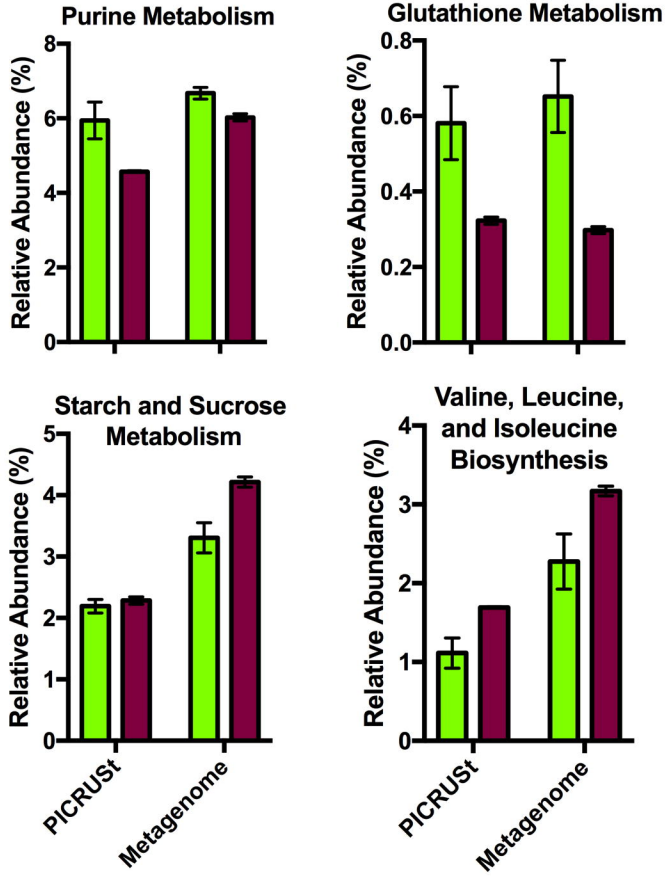
Purine Metabolism
Glutathione Metabolism
Starch and Sucrose Metabolism
Valine, Leucine, and Isoleucine Biosynthesis
Relative Abundance (%)
PICRUSt
Metagenome